A Plugged Trap for Crossed Field Spin-Flip Loss

David Reens, Hao Wu, Tim Langen, and Jun Ye

Physics Department, University of Colorado at Boulder

(Dated: January 29, 2017)

A new electromagnetic trap geometry allows tunable plugging of non-adiabatic spin flip loss in crossed electric and magnetic fields. This loss afflicts a wide set of candidate molecules and operates at much higher temperatures compared with the more familiar atomic spin-flip loss near the zero of a magnetic trap, and thus it's removal represents an important step toward ultracold molecules. Using only an external magnetic bias coil, the loss rate is tuned from over $100~\mathrm{s}^{-1}$ to below the vacuum limited lifetime of $2\mathrm{s}^{-1}$ in a 100 mK sample of OH molecules.

The ultracold regime extends toward molecules on many fronts. Several bialkali molecules are available and others are under development. Creative and carefully engineered laser cooling strategies are tackling certain nearly vibrationally diagonal molecules. A plethora of non-optical cooling strategies have succeeded to greater or lesser extents on other molecules. All of these molecules will require secondary strategies like evaporation or sympathetic cooling to make further gains in phase space density. They also may face a familiar challenge: spin flip loss near the zero of a magnetic trap, but dramatically enhanced for certain molecules. Here we report on our encounter with OH molecule enhanced spin flip loss and our solution.

The knowledge of spin flips or Majorana hops as an eventual trap lifetime limit predates the very first magnetic trapping of neutrals[1]. Spin flips were directly observed and overcome in the TOP trap[2], and shortly later with a plugged dipole trap[3], famously enabling the first Bose-Einstein condensates. The molecular spin-flips can occur at much higher temperatures compared with their atomic counterpart, and thus they need to be addressed much earlier than might have been expected. The magnitude of the loss varies with molecular species, and is particularly strong for the case of the neutral hydroxyl radical (OH) that we study.

Essentially, the loss enhancement is related to the sensitivity of molecules to the relative orientation of E and B fields, whereas in the familiar atomic case it is only the rotation of the magnetic field relative to the lab frame. For Hund's case (a) molecules with very strong spin-rotation coupling, or for case (b) molecules to the extent that their spin-rotation coupling γ is nonzero, electric and magnetic energy shifts add linearly when the fields are parallel but sublinearly when the fields are orthogonal. Consequentially, the presence of a constant orthogonal electric field reduces the magnitude of the Zeeman splitting over a certain range, until the splitting becomes large relative to the influence of the constant electric field. We call this effect "blocking". For the relevant trapped substate of the OH ground state manifold, the Zeeman splitting to the next accessible state is blocked from linear to cubic as shown in fig. 1. The result of this blocking is that when
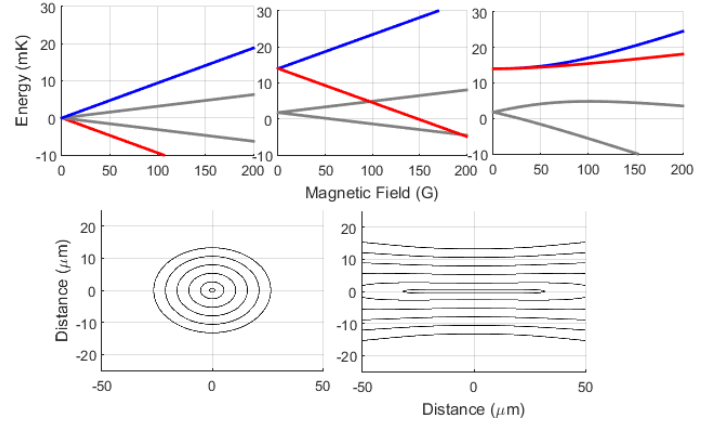

FIG. 1. The blocking effect. (a), four Zeeman split lines in the ground state of OH. A nearly identical set of four states of opposite parity lie 100 mK below. The trapped state and it's spin flip partner are in blue and red. (b) Zeeman splitting with the addition of an electric field of 150 V/cm parallel to the magnetic field. (c) Again but with the fields orthogonal. (d) Contours showing the gap between blue and red states near the zero of a magnetic quadrupole trap without electric field. (e) Again with 150 V/cm. Note the drastic widening of the lowest contour, but without gradient reduction nearby.

$B << E$ and $E \perp B$, the energy gap between states of opposite magnetic quantum number is small, and spin-flips can occur. In a quadrupole trapping geometry with homogeneous electric field, these conditions are met on a disk through the origin whose size is controlled by the magnitude of E. Just outside the disk, blocking returns to linear, which results in a worst case scenario for loss, since $P_{\mathrm{flip}} \propto e^{-\Delta^2/(dE/dt)}$ and we have not only small Δ but large dE/dt. Panel (e) of fig. 1 describes this further.
As panel e shows… disk…

To develop some intuition for this, we work in the basis of total angular momentum and parity which is appropriate for OH's Hund's case (a) ground state. The eight states in this basis are indicated by the state ket $|\epsilon = f, e~;~m_J = \pm 1/2, \pm 3/2\rangle$. An electric field splits states according to the absolute value of their m_J number, with $|f, \pm 3/2\rangle$ shifting upward strongly, $|f, \pm 1/2\rangle$ one third as strongly, and the $|e\rangle$ states shifting oppositely. In the absence of E, the B field would linearly split the states negative parity

according ~~in proportion~~ to m_J, but when the ~~E~~ field has already set the quantization axis with respect to which m_J is defined, an orthogonal ~~B~~ field must first undo the E field's coupling of $|f, 3/2\rangle$ to $|f, -3/2\rangle$, a third order task and thus the cubic dependence of splitting on B. If $E \parallel B$, this basis change is unnecessary and the Zeeman splitting is not blocked. For the $|m_J| = 1/2$ states, realigning the quantization axis when $E \perp B$ is a first order task, so the splitting remains linear; see the gray lines close to zero field in panel (c) of fig. 1.

We can apply Brillouin-Wigner perturbation theory or analytically solve the ground state eigenenergies and taylor expand to obtain the following functional form for the Zeeman splitting between the $|f, \pm3/2\rangle$ states where $E \perp B$:

$$H_Z \approx \frac{(1.4\mu_B B)^3}{(1.7 d_E E)^4}\Delta^2 f(\Delta, d_E E) \tag{1}$$

Here μ_B and d_E are the bohr magneton and the Debye, B and E are the corresponding field magnitudes, Δ is the lambda doublet splitting, and f represents a complicated term of order unity for $d_E E < \Delta$ and order $d_E E/\Delta$ for larger E. We can use this to develop a scaling law for the enhancement. Let κ be the energy threshold for gaps between states below which spin-flips are possible at the 50% level. κ depends on the mean velocity of trapped species and on the trap gradient near the hopping region, and so must be separately computed for any given scenario. For OH molecules in a quadrupole trap [4] with strong gradient 2T/cm and temperature 50mK, $\kappa = 5$MHz. Without electric field, the effective cross sectional area for a hopping region is $\pi\kappa^2$, since loss can occur where $B < \kappa$. With electric field, a much larger B field is required to overcome blocking, so we have from eq. **??** that $B < \sqrt[3]{\frac{\kappa E^4}{\Delta^2}}$, so for $E > \sqrt{\kappa\Delta}$ there is an enhancement given by the following equation:

$$\nu = \left(\frac{E}{\sqrt{\kappa\Delta}}\right)^{\frac{8}{3}} \tag{2}$$

The following table provides numerical values of the loss enhancement factor and absolute rates for various conditions of experimental interest for OH molecules.
How are they calculated?

TABLE I. Enhancements and loss rates for OH

E field	45 mK		20 mK		Purpose
	ν	$\Gamma\,(s^{-1})$	ν	$\Gamma\,(s^{-1})$	
0 V/cm	1	0.1	1	0.4	No Field
300 V/cm	3	0.3	4.7	2.0	Evaporation
550 V/cm	12	1.1	16	6.9	Spectroscopy
3 kV/cm	630	59	840	350	Polarizing

In ref. [5], it was specifically undertaken to investigate the spin-flip loss for OH molecules in a magnetic
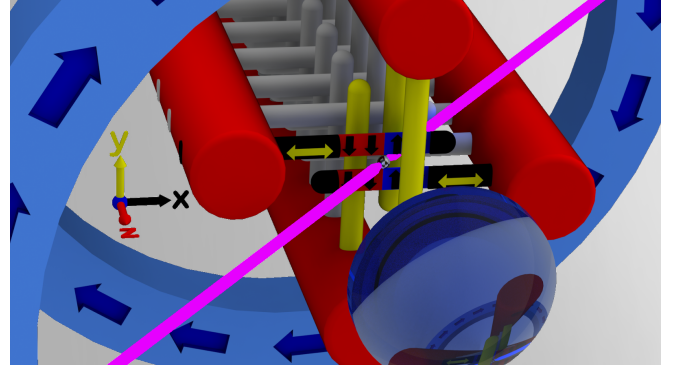

FIG. 2. OH molecules are created using a supersonic expansion source and decelerated from an initial velocity of 460m/s to a final velocity of 40ms/s using a Stark decelerator (red). The decelerator contains 142 electrode pairs (gray). Trapping is achieved by combining a radial magnetic quadrupole field, created by the magnetized second to last electrode pair of the decelerator, with a longitudinal electric quadrupole field created by the third to last and last electrode pairs, respectively (yellow, one electrode is omitted for clarity). The magnetized electrodes can be translated in situ along the x-axis to align their domains and optimize the quadrupole. As there is no trapping magnetic field in the z-direction in this configuration, macroscopic external bias coils can be used to lift the gap between the top two states of the OH ground-state manifold and thus tune the molecular loss. Detection is realized using laser induced fluorescence along the x+y-z direction (blue), which is collected using a lens system and PMT in the z-direction.

Combine this paragraph with other one quadrupole trap with superposed electric field, and no enhancement was found. This turns out to be a consequence of a reasonable yet false assumption that a 4-state approximate Hamiltonian with two spin states and two parities would contain the behavior relevant for spin-flip loss in mixed fields. This approximate Hamiltonian exhibits only constant order blocking- i.e. the Zeeman effect remains linear though with adjusted slope. ~~C.f. the gray $M_J = \pm1/2$ state curves in panel (c) of fig. 1.~~

One obvious way to avoid the loss enhancement is to simply never use electric field in a magnetic trap. This prevents loss from being enhanced compared with atoms, but doesn't remove it entirely. Another possibility is to trap with electric fields, where no spin-flip loss is possible thanks to the $\Delta = 1.67$ GHz splitting between the weak and strong field seeking states. However this splitting also results in a significant reduction in trap gradient close to the center, very undesirable for further cooling by evaporation. Moreover, there are ~~enhancements in elastic collision rates and~~ reductions in inelastic to benefit from in magnetic fields. [6]

Seeking to remove the loss entirely but without trap gradient sacrifice, we switch from a 3D to a 2D magnetic trap, and use an intersecting electric 2D quadrupole to plug the remaining direction (and incidentally add strength to one of the already trapped directions). This does not prevent $E \perp B$, but it allows us to tune the min-
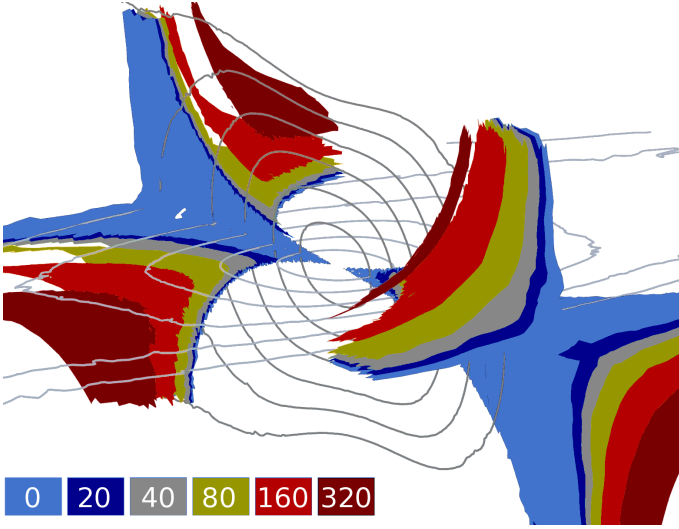
0 20 40 80 160 320

FIG. 3. Each color shows the surfaces where spin-flip can occur for the particular value of B_{coil} given by the legend in units of Gauss. Trap energy contours are shown in gray. Larger B_{coil} pushes the loss regions away from the trap center.

FIG. 4. Family of curves showing the remaining population after 30ms as a function of pin offset and magnetic bias field.

imum B field with an external bias coil oriented along the axis of the 2D quadrupole trap. This is similar to the Ioffe-Pritchard strategy [**?**], where a 2D quadrupole is combined with an axial dipole trap. Typically, the axial and radial trapping interfere somewhat, resulting in significantly lower trap depths. ~~This is averted~~ **we avoid this** by the use of different fields for the axial and radial directions, which can block one another as discussed earlier but never result in an absolute decrease in potential energy of the doubly trapped substate. Serendipitously, we are able to **Add paragraph about our experimental setup?** achieve these fields with a geometry that exactly matches that of our Stark decelerator [7], as shown in fig. 2. By intuition and by our phase space coupling simulations, this represents a near best-case scenario for coupling between a pulsed decelerator and a trap, although in practice we do not realize any significant molecule number increase. This could be related to the difficulty of conditioning the magnet surfaces. For N38 magnets chosen so as to maintain magnetization during violent conditioning procedures, $B' = 5$ T/cm and $E' = 100$ kV/cm^2. These correspond to trap frequencies for a molecule with velocity matching the thermal mean of 7 m/s of $\nu =?$ in each direction. **Calculate the trap freqs.**

Now regarding the molecule enhanced spin-flip loss, $E \perp B$ on a hyperbolic sheet which deviates more significantly from the z axis with increasing B_{coil}, and reduces to the pair of planes $x = 0$ and $y = 0$ in the limit that $B_{coil} = 0$. On this hyperbolic sheet, B must be larger than the threshold set by Eq. 2 to overcome blocking. Fortunately, B_{coil} does not have to overcome the blocking limit, it only needs to push the $B \perp E$ surface slightly off the z-axis for the strong quadrupole fields to overcome
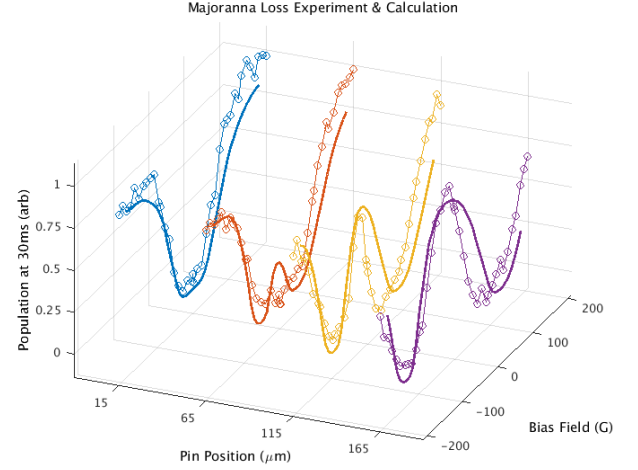
the blocking. In fig. 3, the surfaces where $B \perp E$ are colored wherever the splitting there is below the threshold κ. Since the B fields are more localized than the E, there are always regions susceptible to spin flips, but they can be pushed far enough from the trap center so as to only affect molecules with energy above the trap depth.

In fact, from fig. 3 it would appear that B_{coil} essentially tunes the proximity of the loss regions to the trap center, and that for B_{coil} large enough the loss should be removed. However, translations of our magnetic pins in their mounts lead to important modifications to the **This is true only for perfect pin alignment.** axial behavior of the magnetic trap that must first be addressed. Essentially, when the pairs of magnetic domains of the two pins are out of mutual alignment by a distance d, a small trapping field $\vec{B} \propto B'z\hat{z}d$ is introduced. This means that B_{coil} no longer directly tunes the minimum magnetic field in the trap. Instead, B_{coil} must first overcome the slight trapping field along the z-axis, translating a point of zero field along the z axis and eventually out of the trap. In order to really disentangle this effect from our results, we installed an in-situ pin translation stage and obtained the family of curves shown in fig. 4. With the pins tuned into alignment, B_{coil} does indeed reduce the loss in either direction. Otherwise, B_{coil} first increases the loss by moving the magnetic zero into regions of large electric field, but eventually overwhelms it, hence the characteristic double-well shape.

We fit the family of curves shown in fig. 4 by performing a detailed numerical integration of Landau-Zener hopping probability over all hyperbolic planes where loss can occur, weighted by the expected Maxwell-Boltzmann distribution of molecules in the trap. The computation is performed in COMSOL Multiphysics, with cloud temperature ~~and magnet strength~~ as the only free parame-
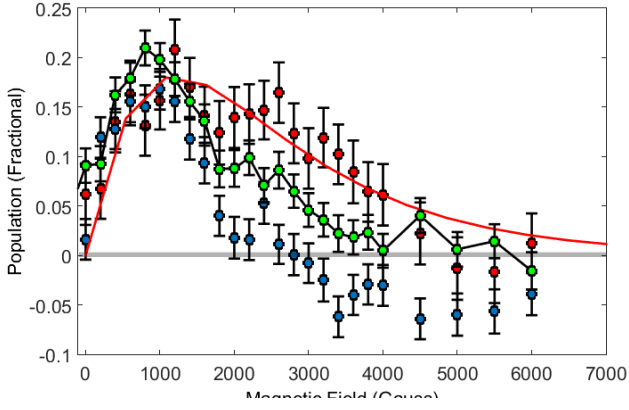
FIG. 5. Microwave Thermometry in the trap.

FIG. 6. Trajectory over time with loss removed, with and without a density reduction technique.

ters. Source-code for the model is available.[?] The fit temperature is 100 ± 10 mK, ~~and the magnetization is 1.2 ± 0.1 T~~, where the uncertainties are chosen so as to keep the fit R^2 within a factor of 2 of the optimal. This temperature is twice that of our previous traps, most likely due to the increased trap depth. ~~The magnetization is consistent with our expectations of the NdFeB magnet grade selected.~~

As a further confirmation of our model for the spin-flip loss in this trapping geometry, we perform a Zeeman microwave spectroscopy along the $|f, 3/2\rangle$ to $|e, 3/2\rangle$ line as in our previous work [6]. Rather than using a bias tee setup, a dangerous ~~operation~~ with our trap deeply integrated in the high voltage decelerator, we use a home-made microwave probe to directly excite free space cavity modes of our vacuum chamber. The results are shown in fig. 5. With the magnetic pins aligned, it is seen that higher values of B_{coil} increase the population of molecules accessing higher magnetic fields in the trap, consistent with our expectation that B_{coil} would tune the distance of the loss region from the trap center. In order to perform this spectroscopy, the trapping electric fields are switched off immediately prior to the application of a microwave transfer pulse tuned to a particular magnetic field strength. Thus the results reflect the Zeeman potential energy only, not the Stark.

In the case of lowest applied magnetic field in fig. 5, i.e. deepest cutting of the loss region toward the trap center, a negative going signal is observed. Since the population signal is obtained via subtractive comparison of molecules in the $|f, 3/2\rangle$ state with and without a microwave coupling to $|e, 3/2\rangle$ applied at a particular B field, this indicates a build-up in the $|e, 3/2\rangle$ state. This suggests a secondary trapped state whose state character has e parity in some regions of the trap. Although the spin-flips we have discussed connect $|f, \pm 3/2\rangle$, the $|f, -3/2\rangle$ state actually remains mostly trapped thanks to adiabatic transitions to $|f, 1/2\rangle$ and later ~~$e, 3/2\rangle$~~ facilitated by the large E fields present in the trap.
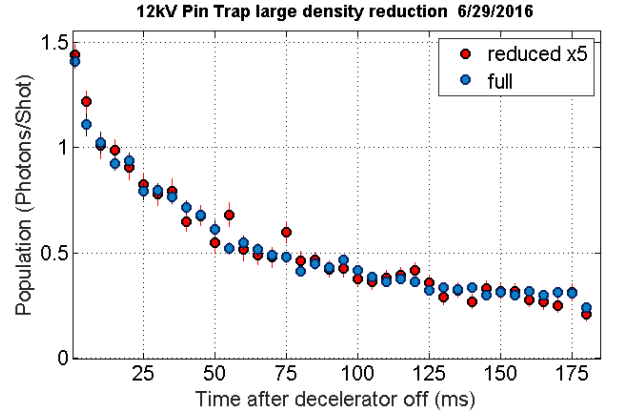
We have conclusively demonstrated the existence of molecule enhanced spin-flip loss by tuning it from an overwhelming rate to complete removal. It remains to be seen what other processes may be in effect once this loss mechanism is removed. Although the trend shown in fig. 6 is suggestive of a collisional process, we implement a completely phase-space blind density reduction technique to significantly reduce our molecule number and observe no change in the trend, indicating that only single particle physics is responsible so far. This is not too surprising given the increased initial temperature of this trap compared to our previous ones, but we intend to address this with a suite of density enhancing experimental improvements in the near term.

$$\vec{B} = B'y\hat{x} + B'x\hat{y} + B_{coil}\hat{z} \tag{3}$$
$$\vec{E} = E'y\hat{y} - E'z\hat{z} \tag{4}$$

$$\vec{B} \cdot \vec{E} = 0 \tag{5}$$
$$B'xE'y - B_{coil}E'z = 0 \tag{6}$$
$$B_{coil}z = xyB' \tag{7}$$

[1] A. L. Migdall, J. V. Prodan, W. D. Phillips, T. H. Bergeman, and H. J. Metcalf, Physical Review Letters **54**, 2596 (1985).
[2] W. Petrich, M. H. Anderson, J. R. Ensher, and E. A. Cornell, Physical Review Letters **74**, 3352 (1995).
[3] K. B. Davis, M. O. Mewes, M. R. Andrews, N. J. van Druten, D. S. Durfee, D. M. Kurn, and W. Ketterle, Physical Review Letters **75**, 3969 (1995).
[4] B. C. Sawyer, B. K. Stuhl, D. Wang, M. Yeo, and J. Ye, Physical Review Letters **101**, 1 (2008).

[5] M. Lara, B. L. Lev, and J. L. Bohn, Physical Review A - Atomic, Molecular, and Optical Physics **78**, 1 (2008), arXiv:arXiv:0806.2245v1.

[6] B. K. Stuhl, M. T. Hummon, M. Yeo, G. Quéméner, J. L. Bohn, and J. Ye, Nature **492**, 396 (2012), arXiv:1209.6343.

[7] J. R. Bochinski, E. R. Hudson, H. J. Lewandowski, J. Ye, and G. Meijer, Physical Review Letters **91**, 5 (2003), arXiv:0306062 [physics].

[8] T. H. Bergeman, P. McNicholl, J. Kycia, H. Metcalf, and N. L. Balazs, Journal of the Optical Society of America B **6**, 2249 (1989).

[9] J. L. Bohn and G. Qu, Molecular physics **111**, 1931 (2013), arXiv:arXiv:1301.2590v1.

[10] R. Golub and J. M. Pendlebury, Reports on Progress in Physics **42**, 439 (1979).

[11] D. E. Pritchard, Physical Review Letters **51**, 1336 (1983).

[12] I. I. Rabi, Physical Review **49**, 324 (1936).

[13] B. K. Stuhl, M. Yeo, M. T. Hummon, and J. Ye, Molecular Physics **111**, 1 (2013).

[14] B. K. Stuhl, M. Yeo, B. C. Sawyer, M. T. Hummon, and J. Ye, Physical Review A - Atomic, Molecular, and Optical Physics **85**, 1 (2012), arXiv:1108.4871.